

A Large-Scale Referring Remote Sensing Image Segmentation Dataset and Benchmark

Zhigang Yang, Huiguang Yao, Linmao Tian, Xuezhi Zhao, Qiang Li, *Member, IEEE*, Qi Wang, *Senior Member, IEEE*

Abstract—Referring Remote Sensing Image Segmentation (RRSIS) is a complex and challenging task that integrates the paradigms of computer vision and natural language processing. Existing datasets for RRSIS suffer from critical limitations in resolution, scene diversity, and category coverage, which hinders the generalization and real-world applicability of refer segmentation models. To facilitate the development of this field, we introduce NWPU—Refer, the largest and most diverse RRSIS dataset to date, comprising 15,003 high-resolution images (1024-2048px) spanning 30+ countries with 49,745 annotated targets supporting single-object, multi-object, and non-object segmentation scenarios. Additionally, we propose the Multi-scale Referring Segmentation Network (MRSNet), a novel framework tailored for the unique demands of RRSIS. MRSNet introduces two key innovations: (1) an Intra-scale Feature Interaction Module (IFIM) that captures fine-grained details within each encoder stage, and (2) a Hierarchical Feature Interaction Module (HFIM) to enable seamless cross-scale feature fusion, preserving spatial integrity while enhancing discriminative power. Extensive experiments conducted on the proposed NWPU-Refer dataset demonstrate that MRSNet achieves state-of-the-art performance across multiple evaluation metrics, validating its effectiveness. The dataset and code are publicly available at <https://github.com/CVer-Yang/NWPU-Refer>.

Index Terms—Remote sensing, benchmark, traffic object, semantic segmentation

I. INTRODUCTION

EXTRACTING Referring segmentation, as a pioneering task at the intersection of computer vision [1], [2] and natural language processing [3], [4], has garnered significant attention due to its ability to segment specific target regions based on user-provided natural language descriptions [5]–[11]. This task is distinguished by its interactivity and flexibility, enabling models to interpret user intent and generate personalized segmentation outcomes. However, the unique characteristics of remote sensing images [12], [13]—including their diverse perspectives, varying scales, and intricate relationships—pose substantial challenges to existing referring segmentation methods.

While the referring segmentation task has garnered significant attention in recent years, existing datasets [14], [15]



Fig. 1. Comparison of refer segmentation datasets for four target categories: bridges, sports fields, ships, and airplanes. As shown in the left column, existing datasets primarily consist of simple scenes with prominent and easily segmented objects. In contrast, our proposed dataset (right column) introduces greater detail and complexity, better capturing the intricate real-world environments encountered in practical applications.

for Referring Remote Sensing Image Segmentation (RRSIS) remain constrained by notable limitations. These datasets are often derived through simplistic secondary processing of existing object detection datasets, which is insufficient to meet the complex and diverse requirements of real-world applications. Consequently, this results in suboptimal data quality and limited diversity. On one hand, annotations in these datasets are frequently generated using automated tools such as the Segment Anything Model (SAM) [16]. Notwithstanding their efficiency, these frameworks are prone to introducing subtle inaccuracies and omitting fine-grained details, which are critical for precise segmentation tasks. On the other hand, as illustrated in Fig. 1, existing datasets predominantly focus on simplified scenarios with salient, isolated targets (e.g., a single ship or a sports field), failing to capture the complexity of real-world remote sensing images. These real-world images typically feature intricate backgrounds and multi-object contexts, which pose significant challenges for accurate segmentation. Furthermore, the relatively outdated nature of the imagery gradually compromises the generalization capabilities of models, thereby undermining their performance in practical applications.

To alleviate these challenges, we undertake a comprehensive, large-scale data collection initiative, amassing remote sensing imagery from diverse geographic regions and scenarios spanning five continents. This extensive dataset captures a broad spectrum of environments, including urban, rural, forested, desert, and oceanic landscapes, thereby ensuring geographic diversity and contextual richness. We further extend

Zhigang Yang, Qiang Li, and Qi Wang are with the School of Artificial Intelligence, Optics and Electronics (iOPEN), Northwestern Polytechnical University, Xi'an 710072, P.R. China. (e-mail: zgyang@mail.nwpu.edu.cn, liqmgcs@gmail.com, crabwq@gmail.com)

Huiguang Yao is with School of Computer Science, Northwestern Polytechnical University, Xi'an 710072, P.R. China. (e-mail: yhg2655@mail.nwpu.edu.cn)

Linmao Tian and Xuezhi Zhao are with the department of Software, Northwest Institute of Nuclear Technology, Xi'an 710072, P.R. China. (e-mail: tianlm0808@mail.nwpu.edu.cn, xuezhizhao@mail.nwpu.edu.cn)

the task definition by pioneering the introduction of category-based referring expressions in RRSIS, enabling users to specify broader object categories (e.g., “all vehicles”, “the first row of photovoltaic panels”, or “vehicles traveling left on the road”) and accommodate no-target scenarios. This innovation markedly enhances the task’s flexibility and applicability while presenting a more demanding research direction for future exploration. In addition, we introduce MRSNet, a novel remote sensing referring segmentation network designed to effectively handle the complexities of RRSIS. MRSNet integrates both intra-scale and cross-scale feature interactions to ensure robust feature extraction and aggregation. At each encoder stage, an intra-scale feature interaction module is employed to capture features of targets across varying scales and model their interrelationships. Moreover, a hierarchical feature interaction module is implemented to facilitate efficient cross-scale feature aggregation while preserving feature integrity. The principal contributions of this work are encapsulated as follows:

- We present referring remote sensing image segmentation dataset of global scale, which includes a variety of geographic and environmental scenarios across five continents. This dataset captures the complexities of real-world applications and introduces new tasks such as multi-target and no-target scenarios, thus broadening the scope of RRSIS and better meeting the demands of practical applications.
- We propose a multi-scale referring segmentation network meticulously designed to tackle the complexities of RRSIS tasks. At each encoder stage, the network employs an intra-scale feature interaction module to effectively capture multi-scale target details, spatial relationships between targets, and text-selectively aligned visual features. Additionally, a hierarchical feature interaction module is integrated to ensure efficient feature integration, thereby enhancing segmentation accuracy while preserving feature consistency.
- Extensive experiments are conducted to evaluate the proposed method across a wide range of scenarios. The results demonstrate substantial performance improvements compared to existing approaches, confirming the effectiveness of the proposed work.

II. RELATED WORK

In this section, we review the relevant datasets and refer segmentation methods.

A. Reference Image Segmentation Datasets

The development of referring segmentation has been significantly propelled by numerous high-quality datasets [17], [18]. Among these, the RefCOCO dataset [19], an extension of the MSCOCO dataset [20], provides annotations specifically designed for referring segmentation. This dataset facilitates the exploration of the intricate relationships between language descriptions and visual targets by integrating language and vision modalities. Building upon this foundation, the gRefCOCO dataset [6] extends the scope of referring expressions to include descriptions referencing multiple targets within a single

image, thereby enhancing its representativeness for real-world applications. In the domain of remote sensing imagery, the RSIS dataset stands as the first benchmark explicitly developed for referring segmentation. It leverages the Segment Anything Model (SAM) [16] to generate segmentation masks from the RSVGD dataset [21], paired with corresponding natural language descriptions. Despite these advancements, existing remote sensing datasets exhibit notable limitations. These datasets predominantly focus on salient objects, limiting their ability to address challenging scenarios involving small or low-contrast targets. Furthermore, the image sources lack temporal and spatial diversity, often being restricted to outdated scenes with limited complexity. Additionally, the annotations are primarily in English, which hinders their applicability in multilingual regions and reduces their relevance to diverse real-world applications. To address these limitations, we propose a large-scale bilingual referring segmentation dataset for remote sensing imagery. This dataset enables precise identification and localization of various targets, adapts to complex scenarios, and enhances task diversity and practicality.

B. Referring Image Segmentation Methods

Building on the foundations laid by these datasets, researchers [22]–[27] have proposed various methods for language-guided referring segmentation [28]–[31] and reasoning segmentation [32]–[34]. Early approaches [35]–[37] primarily rely on convolutional neural network (CNN) based architectures, where multimodal fusion is achieved through simple concatenation of language embeddings and image features. For instance, the CMSA model [38] introduces cross-modal self-attention mechanisms to compute similarities between language descriptions and image regions, generating initial segmentation results. However, these methods often struggle with limited fusion capabilities, making it challenging to capture the complex contextual information embedded in language descriptions.

Transformer-based approaches [39] have brought significant advancements to this field. For example, the Language-Aware Vision Transformer (LAVT) [40] enables deep interaction between language embeddings and image features, effectively capturing fine-grained semantics in language descriptions. This improves the understanding of complex linguistic instructions and enhances segmentation accuracy. Similarly, the RMSIN model integrates multiple visual and linguistic gating mechanisms to align features, while its adaptive rotational convolutions in the decoder ensure precise segmentation of referred objects. Despite these advancements, substantial challenges remain. Remote sensing images encompass a wide range of object scales, from large targets such as ground tracks to small objects like vehicles that occupy only a few pixels. This necessitates models that can effectively perceive and represent features across multiple scales. Furthermore, remote sensing referring segmentation tasks demand enhanced positional sensitivity, requiring models to accurately capture spatial relationships, including vertical and horizontal distinctions. Additionally, certain scenarios involve the absence of target objects, necessitating models to selectively align visual and

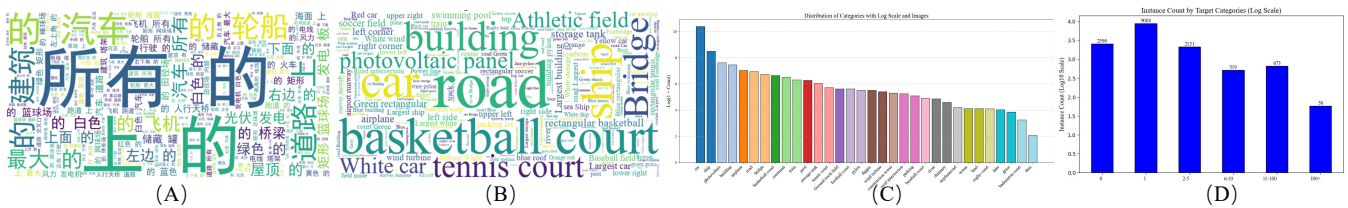


Fig. 2. Illustration of data distribution characteristics.

linguistic features to achieve robust segmentation. Cross-scale feature aggregation [41], [42] has demonstrated substantial benefits in segmentation tasks by enabling effective feature modeling and integration. Incorporating cross-scale feature aggregation into remote sensing referring segmentation offers a promising direction for improving feature representation and segmentation performance. This approach not only addresses the challenges posed by multi-scale objects but also enhances the model’s ability to handle complex spatial relationships and diverse scenarios.

C. Dataset Annotation

To ensure precise and high-quality data annotations, a systematic process is designed with three key components.

Step 1: Target category definition. A comprehensive set of 32 target categories commonly observed in remote sensing imagery is defined to ensure diverse and structured representation. These categories include transportation targets such as cars, ships, trains, and airplanes; infrastructure including bridges, roads, road intersections, buildings, and airport runways; natural and artificial scenes such as lakes, rivers, grasslands, open areas, and oceans; sports facilities including basketball courts, ground track fields, soccer fields, and tennis courts; industrial equipment such as wind turbines, power line towers, storage tanks, and construction towers; and other objects including parking lots, dams, chimneys, and containers.

Step 2: Multi-language Annotation. To support personalized and diverse referring segmentation tasks, annotations are created across six dimensions: size-based references, spatial relationships, color attributes, category relations, motion states, associative relationships.

Step 3: Data Labeling and Quality Assurance. A team of four experts conducts the annotation process. Three trained annotators label target categories, attributes, and spatial relationships, while a senior annotator reviews the dataset for completeness, accuracy, and consistency. All annotations are manually performed without auxiliary tools, ensuring high precision and reliability.

D. Dataset Analysis

The NWPU-Refer dataset is a comprehensive resource for remote sensing image segmentation, featuring a diverse collection of images with resolutions ranging from 0.12m to 0.5m. This high-resolution imagery captures a wide variety of remote sensing scenarios, making it an ideal benchmark for evaluating the performance of segmentation models in complex environments. Fig.2(A) and Fig.2(B) provide word clouds

generated from the annotations, offering a visual summary of the most frequently mentioned terms in the dataset. These word clouds highlight common targets such as cars, ships, and airplanes, which dominate the majority of instances. In contrast, rarer targets like badminton courts, dams, and golf courses are less frequently mentioned, indicating their smaller proportion within the dataset.

Fig.2(C) illustrates the distribution of annotation categories, showing that common targets account for a significant portion of the dataset. For instance, cars and ships make up the largest categories, while badminton courts and dams represent only a small fraction. This imbalance in category distribution poses challenges for model training, as it requires the model to effectively generalize across both frequent and rare categories.

Furthermore, Fig.2(D) presents the distribution of annotation types, revealing that single-target descriptions are the most prevalent, accounting for the majority of annotations. Multi-target descriptions are less common, while descriptions without specific targets are the least frequent. This distribution suggests that models trained on this dataset should be optimized to handle single-target scenarios efficiently while also being capable of managing more complex multi-target situations.

E. Typical Scene Analysis

To intuitively demonstrate the diversity of the dataset, we conduct a visual analysis of each annotated object category. As shown in Fig.3, the targets in the dataset exhibit significant diversity and complexity, including buildings of various shapes, vehicles of different sizes, and vehicle categories with intricate relationships. In addition, we analyze special cases in the dataset, such as occluded targets and blurry target scenarios. In these cases, the boundaries of the targets are ambiguous, or their semantics are unclear, posing greater challenges to the segmentation accuracy of models. However, these challenging samples also provide valuable opportunities for evaluating model performance in complex scenarios.

F. Comparison with Existing Datasets

Table I compares three remote sensing referring segmentation datasets: RefSegRS, RRSIS-D, and the proposed NWPU-Refer, focusing on resolution, dataset size, annotation types, and methods. RefSegRS contains 4,420 images at 0.13m resolution with manually generated annotations, but its limited size and annotation diversity restrict its applicability to complex scenarios. RRSIS-D offers a larger dataset of

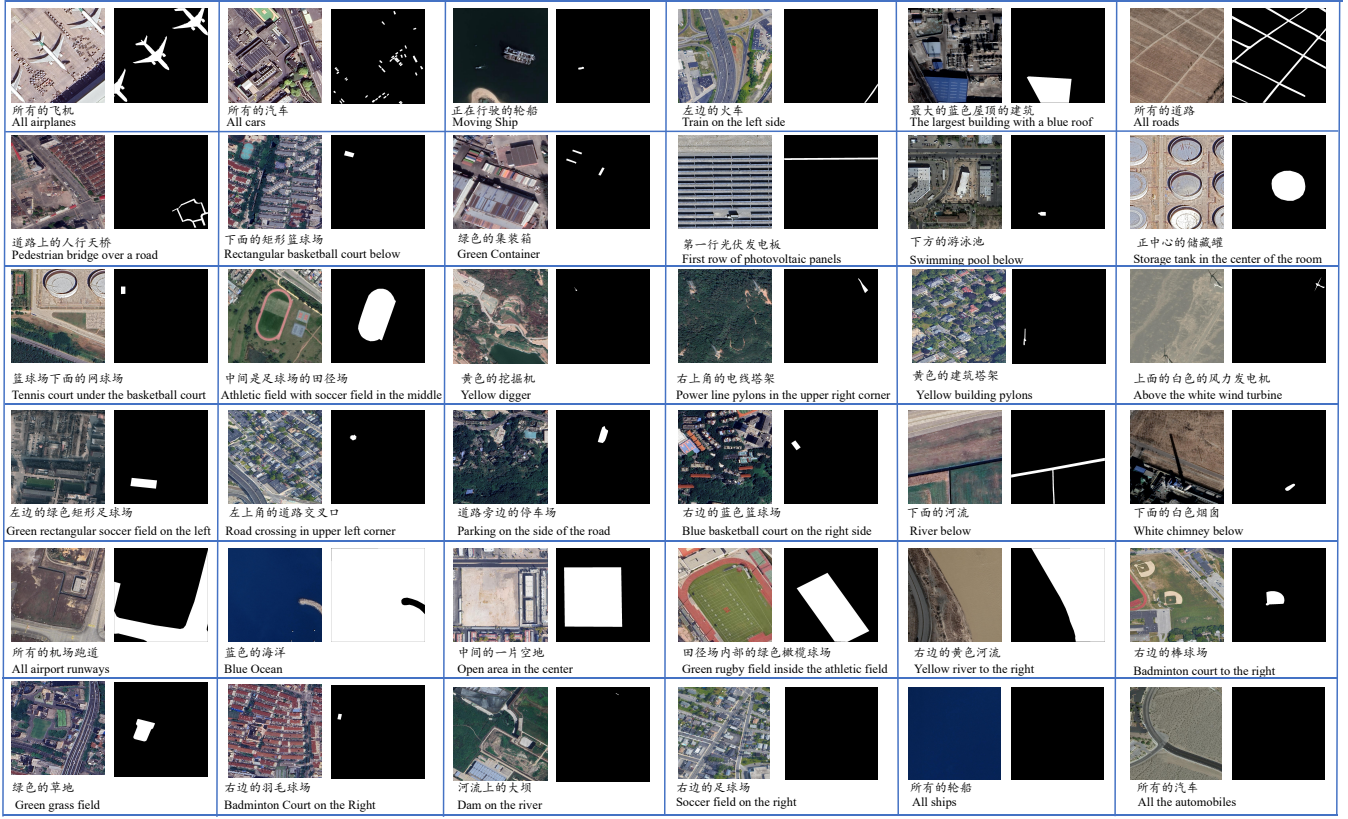


Fig. 3. Example visualizations of the NWPU-Refer.

TABLE I
THE COMPREHENSION WITH THE EXISTING DATASETS.

Dataset	Image Resolution	Images	Annotations	Single-object	Multi-object	Non-Object	Resolution	Annotation Generation
RefSegRS	0.13m	4420	4420	✓	×	×	512	Manual
RRSIS-D	0.5m–30m	17402	17402	✓	×	×	800	Semi-auto
NWPU-Refer	0.12m–0.5m	15003	49745	✓	✓	✓	1024–2048	Manual

17,402 images with resolutions from 0.5m to 30m but relies on semi-automatic annotations. In contrast, NWPU-Refer comprises 15,003 images with resolutions between 0.12m and 0.5m, preserving detailed spatial information. It includes 49,745 manually generated annotations, covering no-target and multi-target scenarios, ensuring precision and reliability. With high-resolution imagery, diverse annotation types, and manual verification, NWPU-Refer provides a robust resource for advancing research in complex segmentation tasks.

III. METHODS

A. Overview

The architecture of our proposed MRSNet is depicted in Fig. 4, comprising three core components: the Intra-scale Feature Interaction Module (IFIM), the Hierarchical Feature Integration Module (HFIM), and the decoder. We utilize the Swin-Transformer [43] as the backbone for visual feature extraction and the BERT network [44] as the backbone for linguistic feature extraction.

At the initial stage, a remote sensing image $I \in \mathbb{R}^{H \times W \times 3}$ and a language description $L \in \mathbb{R}^{N \times C}$ are fed into the model. The IFIM is integrated into each stage of the encoder to enhance the alignment between visual features and linguistic semantics. The HFIM aggregates features across different scales to generate a comprehensive feature representation. Finally, the decoder, which follows the configuration in [15], refines these integrated features to produce precise segmentation masks corresponding to the input language description.

B. Intra-Scale Feature Interaction Module

The Intra-Scale Feature Interaction Module is designed to perform three key functions: capturing multi-scale visual features, modeling contextual relationships between targets, and achieving visual-linguistic alignment. This module enhances feature completeness and discriminability, significantly advancing complex scene referring segmentation capabilities.

a) Pyramidal Spatial-Spectral Refinement Submodule:

As shown in Fig. 5, the visual feature map is refined in both spatial and frequency domains across multiple scales,

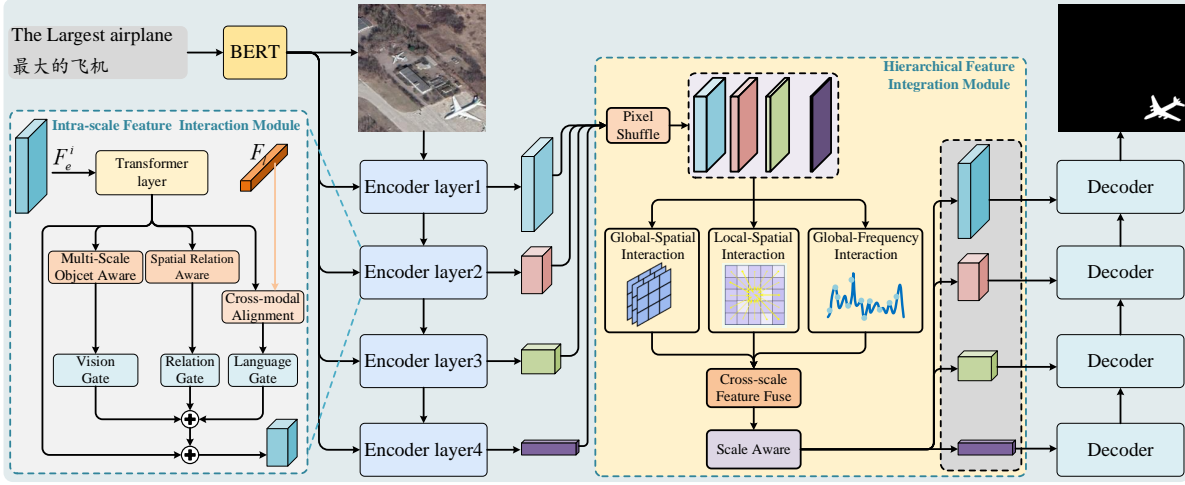


Fig. 4. The overview of the proposed MRSNet.

generating comprehensive feature representations with robust intra-scale perception. This is particularly important for handling objects of different scales in remote sensing images. *Spatial-Spectral Refinement*: Given the input feature map

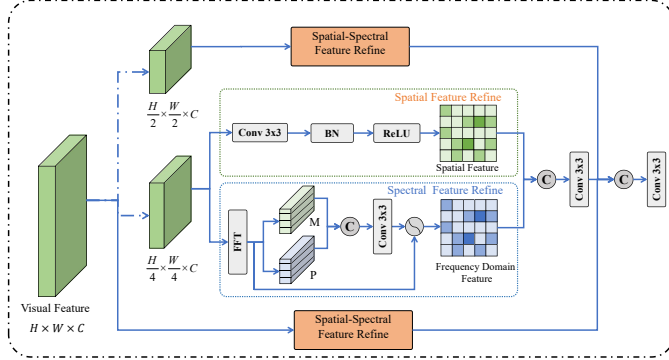


Fig. 5. The structure of the proposed pyramidal spatial-spectral refinement submodule.

$X \in \mathbb{R}^{B \times N \times \dim}$, it is reshaped into a feature map $X_{2D} \in \mathbb{R}^{B \times \dim \times H \times W}$, where $H \times W = N$. Then, a spatial refined feature X_s is generated through a convolution operation. Simultaneously, a Fourier Fast Transform is applied to X_{2D} to extract the frequency domain magnitude M and phase P . These components are concatenated and processed through a convolution layer followed by a softmax activation to generate frequency weights:

$$W_f = \text{Softmax}(\text{Conv}([M, P])) \odot X_{2D},$$

where \odot denotes element-wise multiplication. The frequency domain features X_f are then obtained by applying these weights to X_{2D} . Finally, the spatial features X_s and frequency domain features X_f are fused through concatenation followed by a convolution operation to produce the refined feature map. These weights are applied to X_{2D} using element-wise multiplication to generate the frequency domain features X_f . Finally, the spatial features X_s and the frequency domain features X_f are fused through concatenation, followed by a convolution operation.

Pyramidal Feature Aggregation: To capture multi-scale target features, the input feature map is downsampled by factors of 2 and 4, resulting in low-resolution feature maps $X_{2D}^{1/2}$ and $X_{2D}^{1/4}$, respectively. At each scale, spatial and frequency domain attention features are extracted and fused using the aforementioned *Spatial-Spectral Refinement* process. The aggregated features are upsampled to the original resolution and concatenated to form the final pyramidal feature map F_{py} .

b) *Context-Aware Spatial Relation Modeling Submodule*: For the refer segmentation tasks, which require capturing relationships between target objects, this submodule is designed to extract interactions between targets. As shown in Fig. 6, starting with the input feature map $X_{2D} \in \mathbb{R}^{B \times \dim \times H \times W}$, a spatial adjacency matrix $A \in \mathbb{R}^{N \times N}$ is constructed to represent the connectivity between each pixel and its surrounding neighbors, defined as:

$$A_{ij} = \begin{cases} 1, & \text{if } j \text{ is a neighbor of } i; \\ 0, & \text{otherwise.} \end{cases}$$

To ensure consistent information propagation, the adjacency matrix A is row-normalized such that the sum of each row equals 1, standardizing the influence of neighboring pixels.

Feature Aggregation between Points: Using the adjacency matrix A , the flattened input features $X_{\text{flat}} \in \mathbb{R}^{B \times \dim \times N}$ are aggregated with the neighborhood features to generate contextual features. This operation effectively aggregates neighborhood information into each pixel, enhancing contextual understanding, particularly for pixels strongly correlated with their targets.

Graph Convolution and Feature Update: The contextual features C_{context} are processed through a graph convolution network to capture pixel-wise relationships while maintaining spatial and semantic consistency. The output feature F_{GCN} is then passed through a convolution layer to produce the refined features $F_{\text{relationship}}$.

c) *Cross Model Align Submodule*: This submodule is designed to selectively align visual features with textual features. By incorporating a pixel-wise adaptive fusion mechanism, it

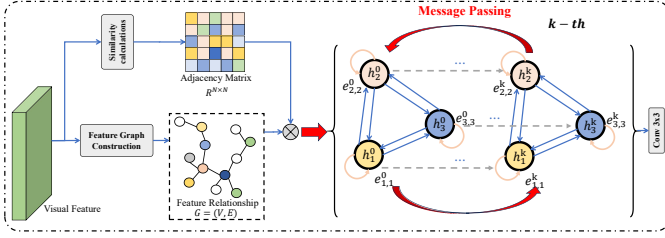


Fig. 6. The structure of the proposed context-aware spatial relation modeling submodule.

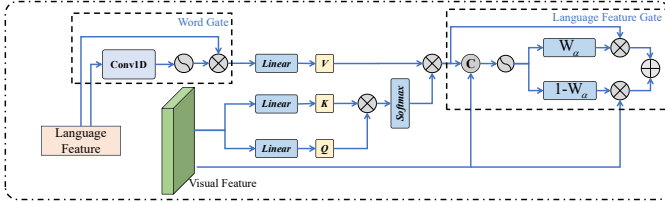


Fig. 7. The structure of the proposed Cross Model Align Submodule.

effectively integrates visual and language features, playing a crucial role in referential segmentation tasks. The structure of this submodule is shown in Fig. 7.

Image-Language Interaction: The input visual feature X_{2D} is first projected through a 1D convolution followed by an activation function, producing transformed visual features $V_{\text{proj}} \in \mathbb{R}^{B \times \text{dim} \times N}$. To model semantic relationships between visual and linguistic features, the image-language interaction mechanism proceeds as follows: The projected visual features X_{proj} are mapped into queries Q , while the linguistic features $L \in \mathbb{R}^{B \times L_{\text{in}} \times N_l}$ are mapped into keys K and values V . A dynamic language importance weight G_{lang} is calculated to represent the semantic relevance of each word:

$$G_{\text{lang}} = \sigma(\text{Conv1D}(L)),$$

where σ denotes the Sigmoid activation function. Subsequently, the input words are weighted by applying these weights to enhance the semantic representation of the linguistic features. Cross-modal relationships are captured by computing the similarity between visual queries Q and linguistic keys K , resulting in an attention map S . The attention map S is then used to weight the linguistic values V , producing the enhanced visual features V_L that are aligned with the linguistic features. The attended linguistic features V_L are projected to match the input visual features for subsequent fusion.

Cross Model Feature Fusion. The projected visual features V_{proj} and the attended visual features V_L are concatenated along the channel dimension to form fused features. An attention mechanism is employed to compute the fusion weights W_{proj} , which are then applied to combine these features :

$$F_{\text{cm}} = W_{\text{proj}} \cdot V_{\text{proj}} + (1 - W_{\text{proj}}) \cdot V_L.$$

The fused features are projected through a 1D convolution to produce the final cross-modal feature representation F_{cm} .

d) Adaptive Feature Fusion Module: The feature maps F_{py} , $F_{\text{relationship}}$, F_{cm} are concatenated along the channel dimension. A gated mechanism is applied to compute

the respective weights for these feature maps using linear transformations, Sigmoid activation, and split operations. The weighted feature maps are then fused through element-wise addition and linear transformations, resulting in the refined feature map for this stage.

C. Hierarchical Feature Integration Module

To address the challenge of integrating multi-scale feature information in complex visual tasks, we propose a Hierarchical Feature Integration Module (HFIM). This module ensures the integrity of feature information by redistributing channel information into spatial dimensions through a PixelShuffle operation. The generated intermediate feature maps are concatenated along the channel dimension to form a unified feature representation. Furthermore, HFIM leverages depthwise separable convolutions, spatial self-attention, and frequency self-attention to achieve comprehensive multi-scale feature fusion and efficient encoding across spatial and frequency domains.

a) Spatial domain feature Integration: To extract spatial features, the input features are first processed through depthwise separable convolutions, batch normalization (BN), and ReLU activation. This process efficiently captures local neighborhood information, producing local features F_{local} .

To capture global features, we employ a multi-head self-attention mechanism. The input feature map is first projected into three distinct spaces to derive queries, keys, and values. The attention scores are computed by measuring the similarity between queries and keys, followed by a softmax operation to obtain normalized attention weights. These weights are subsequently applied to the values to generate the global features F_{global} .

b) Frequency Domain Feature Integration: To capture global frequency information, the input features are transformed into their frequency domain representation F_{freq} using a Fast Fourier Transform. In this domain, normalized similarities between the query Q_f and key K_f are computed, and the value V_f are weighted to generate frequency-domain features:

$$F_{\text{freq}} = \text{IFFT} \left(\text{Softmax} \left(\frac{Q_f \cdot K_f^\top}{\sqrt{d_k}} \right) \cdot V_f \right).$$

The resulting frequency features are transformed to the spatial domain through an inverse Fourier transform, yielding $F_{\text{freq}} \in \mathbb{R}^{B \times C \times H \times W}$.

c) Feature Fusion: The F_{local} , F_{global} , F_{freq} are concatenated along the channel dimension to form the unified feature F_{fuse} . Then, a 1×1 convolution is then applied to reduce the channel dimensionality, resulting in the final fused feature.

d) Hierarchical Feature Division: To integrate multi-scale features from the encoder, PixelUnshuffle operations are applied to align the spatial resolutions of all feature maps. After aligning the resolutions, the fused features are split according to their original channel dimensions and restored to their respective scales. This hierarchical integration process allows the model to leverage fine-grained details while maintaining a global context, ensuring consistent multi-scale feature representation.

TABLE II
PERFORMANCE COMPARISON ACROSS METHODS. THE BEST RESULTS ARE IN BOLD.

Method	P@0.7		P@0.8		P@0.9		oIoU		mIoU	
	val	test	val	test	val	test	val	test	val	test
LAVT	25.22	23.29	17.16	15.50	7.31	6.92	62.23	55.61	34.66	33.90
RMSIN	31.51	32.03	20.37	19.92	9.50	7.70	62.66	55.64	41.75	43.52
MRSNet	33.01	30.90	22.08	20.47	9.23	8.54	63.59	57.04	44.86	43.60

IV. EXPERIMENT

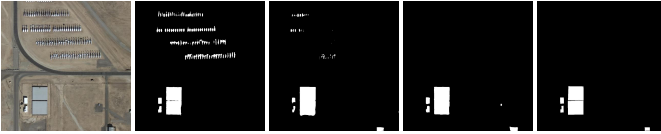
A. Dataset Setup and Evaluation Metrics

The dataset is divided into training, validation, and test sets using a 7:1:2 ratio based on the sample distribution across different regions. To comprehensively evaluate the performance of the model, the following metrics are selected: precision at thresholds (P@0.7, P@0.8, P@0.9), overall IoU (oIoU), and mean IoU (mIoU).

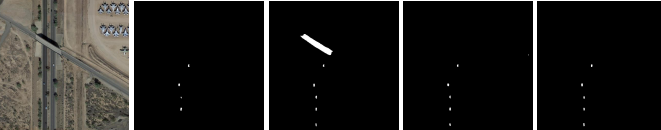
B. Experimental Settings

All experiments are performed using PyTorch and trained on an NVIDIA GTX 6000 GPU. The AdamW optimizer is employed with an initial learning rate of $6e-4$, and a cosine annealing strategy is used to dynamically adjust the learning rate, facilitating faster convergence. To ensure fair comparisons, only the English language is used for training.

Text: All buildings.



Text: Cars on the road.



Text: Train on the tracks.

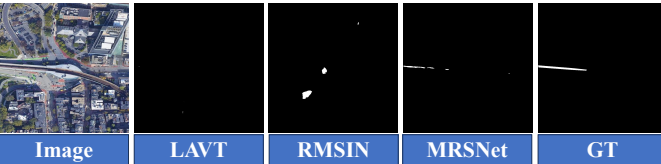


Fig. 8. Qualitative comparisons between MRSNet, LAVT and RMSIN.

C. Comparison with Existing Methods

To evaluate the performance of the proposed MRSNet model, we compare it with two widely adopted methods, LAVT and RMSIN, across multiple evaluation metrics, as shown in Table II. MRSNet consistently outperforms these baselines, achieving state-of-the-art results in precision at thresholds (P@0.7, P@0.8, P@0.9), oIoU, and mIoU. For example, at P@0.8, MRSNet achieves 22.08% and 20.47% on the validation and test sets, respectively, outperforming RMSIN by 1.71% and 0.55%. The significant performance gains of MRSNet can be attributed to its architectural innovations. The intra-scale feature interaction module effectively

enhances feature representation at each encoder stage by aligning detailed spatial and semantic information. Simultaneously, the hierarchical feature integration module ensures efficient cross-scale feature fusion, enabling the model to capture both fine-grained details and global context. The intra-scale feature interaction module enhances the capture of detailed features at each encoder stage, while the hierarchical feature interaction module facilitates efficient cross-scale feature integration. These modules enable MRSNet to achieve higher oIoU and mIoU compared to RMSIN and LAVT, demonstrating its ability to handle diverse and challenging segmentation tasks. Overall, these results highlight the capability of model to address key limitations in existing methods. By effectively integrating multi-scale features and aligning visual and linguistic representations, MRSNet sets a new benchmark for referring RRSIS.

D. Visual Results

As shown in Fig.8, our model demonstrates superior reasoning capabilities compared to other methods in challenging scenarios. In the first row, our model accurately localizes the building based on the language description, whereas the other models incorrectly identify airplanes as a building. In the second row, our model achieves a more precise and complete segmentation of the car, better preserving its shape and boundaries. In the third row, our model successfully localizes the train target, while the other methods exhibit significant inaccuracies. These observations highlight the robustness of our model in aligning textual descriptions with visual features, ensuring accurate segmentation and localization in complex remote sensing tasks.

E. Visualization Results of Chinese Referring Segmentation

As illustrated in Fig.9, we provide some Chinese language-guided segmentation visualization results in the NWPU-Refer dataset. The majority of the textual prompts used in the experiments are self-designed, reflecting the model's adaptability to user-defined queries. In the single-object segmentation task, the model accurately identifies specific objects such as a white airplane on the runway, a bridge over a river, and a ship at sea. The segmentation masks effectively delineate the contours of the target objects, highlighting the model's robust localization capabilities under varying background and lighting conditions. For multi-object segmentation, the model exhibits strong performance in handling multiple instances. It successfully segments all swimming pools, airplanes, and vehicles on the road, demonstrating its ability to maintain consistent accuracy regardless of variations in object size, quantity, and

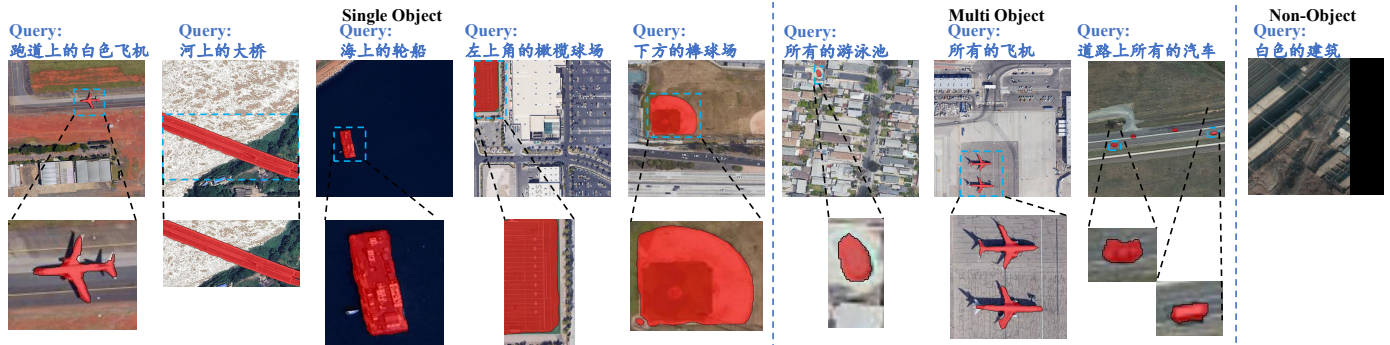


Fig. 9. The visualization results of MRSNet for Chinese referring expression segmentation. The left section showcases predictions for Single objects, the middle section showcases predictions for Multi objects, and the right demonstrates performance on Non objects.

spatial distribution. Additionally, the non-object segmentation results underscore the model’s semantic comprehension and exclusion capabilities. When queried to identify “white buildings,” the model produces no predictions, indicating its ability to disregard irrelevant regions and adhere strictly to the query description. Overall, these results emphasize the model’s robustness and accuracy in addressing diverse segmentation tasks. Its ability to generalize across varied object types, scales, and background complexities underscores its strong applicability to real-world scenarios.

F. Ablation Study

To validate the efficacy of our proposed multi-scale feature extraction and target relationship modeling in IFIM, we conduct ablation studies on all combinations of pyramidal spatial-spectral refinement (PSR) and Context-Aware Spatial Relation Modeling (CSR). As illustrated in Tabel III, the introduction of PSR brings about significant improvements in precision, especially at higher IoU thresholds, while the incorporation of CSR further refines the target relationships, enhancing the performance across various evaluation metrics. The combined effect of both modules demonstrates a synergistic enhancement, yielding the highest performance across all evaluated metrics, particularly in P@0.7, P@0.8, and mIoU, with margins ranging from 5% to 7%. These findings confirm the critical role played by PSR and CSR in capturing multi-scale features and modeling target relationships, thus substantiating their efficacy in advancing overall segmentation performance.

TABLE III
PERFORMANCE RESULTS FOR DIFFERENT PSR AND CSR CONFIGURATIONS ON TEST DATASET.

PSR	CSR	P@0.7	P@0.8	P@0.9	oIoU	mIoU
✓	×	21.57	12.51	4.35	48.04	36.82
×	✓	23.18	16.21	6.16	52.10	40.08
✓	✓	30.90	20.47	8.54	57.04	43.60

V. CONCLUSION

In this paper, we introduce a large-scale RRSIS dataset, named NWPU-Refer, which offers significant advantages in

data scale and scene diversity compared to existing RRSIS datasets. Additionally, the incorporation of bilingual annotations enhances its application potential, making it a valuable resource for cross-lingual vision-language research. We also present the **Multi-scale Referring Segmentation Network (MRSNet)**, a sophisticated model designed to address the challenges of RRSIS. MRSNet effectively extracts object features and their interrelationships across different scales through the use of an Intra-scale Feature Interaction Module at each encoder stage. Furthermore, a Hierarchical Feature Interaction Module is designed to ensure comprehensive integration of global semantic information and local detailed features, enabling the model to handle complex spatial variations and intricate object relationships. Extensive experiments on the proposed NWPU-Refer dataset demonstrate that MRSNet achieves state-of-the-art performance, setting a new benchmark for future research in this field.

REFERENCES

- [1] Z. Wei, L. Chen, Y. Jin, X. Ma, T. Liu, P. Ling, B. Wang, H. Chen, and J. Zheng, “Stronger fewer & superior: Harnessing vision foundation models for domain generalized semantic segmentation,” in *Proceedings of the IEEE/CVF conference on computer vision and pattern recognition*, 2024, pp. 28 619–28 630.
- [2] B. Xie, J. Cao, J. Xie, F. S. Khan, and Y. Pang, “Sed: A simple encoder-decoder for open-vocabulary semantic segmentation,” in *Proceedings of the IEEE/CVF conference on computer vision and pattern recognition*, 2024, pp. 3426–3436.
- [3] H. Zhi, P. Chen, J. Li, S. Ma, X. Sun, T. Xiang, Y. Lei, M. Tan, and C. Gan, “Lscenellm: Enhancing large 3d scene understanding using adaptive visual preferences,” *arXiv preprint arXiv:2412.01292*, 2024.
- [4] D. Di Palma, “Retrieval-augmented recommender system: Enhancing recommender systems with large language models,” in *Proceedings of the 17th ACM Conference on Recommender Systems*, 2023, pp. 1369–1373.
- [5] H. Huang, S. Xie, L. Lin, Y. Iwamoto, X. Han, Y.-W. Chen, and R. Tong, “Scaleformer: revisiting the transformer-based backbones from a scale-wise perspective for medical image segmentation,” *arXiv preprint arXiv:2207.14552*, 2022.
- [6] C. Liu, H. Ding, and X. Jiang, “Gres: Generalized referring expression segmentation,” in *Proceedings of the IEEE/CVF conference on computer vision and pattern recognition*, 2023, pp. 23 592–23 601.
- [7] C. Shang, Z. Song, H. Qiu, L. Wang, F. Meng, and H. Li, “Prompt-driven referring image segmentation with instance contrasting,” in *Proceedings of the IEEE/CVF Conference on Computer Vision and Pattern Recognition*, 2024, pp. 4124–4134.
- [8] Y. X. Chng, H. Zheng, Y. Han, X. Qiu, and G. Huang, “Mask grounding for referring image segmentation,” in *Proceedings of the IEEE/CVF Conference on Computer Vision and Pattern Recognition*, 2024, pp. 26 573–26 583.

- [9] H. Ding, C. Liu, S. He, X. Jiang, and C. C. Loy, “Mevis: A large-scale benchmark for video segmentation with motion expressions,” in *Proceedings of the IEEE/CVF international conference on computer vision*, 2023, pp. 2694–2703.
- [10] L. Karazija, I. Laina, and C. Rupprecht, “Clevrtex: A texture-rich benchmark for unsupervised multi-object segmentation,” *arXiv preprint arXiv:2111.10265*, 2021.
- [11] D. Z. Chen, A. X. Chang, and M. Nießner, “Scanrefer: 3d object localization in rgb-d scans using natural language,” in *European conference on computer vision*. Springer, 2020, pp. 202–221.
- [12] Q. Li, W. Zhang, W. Lu, and Q. Wang, “Multi-branch mutual-guiding learning for infrared small target detection,” *IEEE Transactions on Geoscience and Remote Sensing*, 2025.
- [13] Q. Li, M. Zhang, Z. Yang, Y. Yuan, and Q. Wang, “Edge-guided perceptual network for infrared small target detection,” *IEEE Transactions on Geoscience and Remote Sensing*, 2024.
- [14] Z. Yuan, L. Mou, Y. Hua, and X. X. Zhu, “Rrsis: Referring remote sensing image segmentation,” *IEEE Transactions on Geoscience and Remote Sensing*, 2024.
- [15] S. Liu, Y. Ma, X. Zhang, H. Wang, J. Ji, X. Sun, and R. Ji, “Rotated multi-scale interaction network for referring remote sensing image segmentation,” in *Proceedings of the IEEE/CVF Conference on Computer Vision and Pattern Recognition*, 2024, pp. 26658–26668.
- [16] A. Kirillov, E. Mintun, N. Ravi, H. Mao, C. Rolland, L. Gustafson, T. Xiao, S. Whitehead, A. C. Berg, W.-Y. Lo *et al.*, “Segment anything,” in *Proceedings of the IEEE/CVF International Conference on Computer Vision*, 2023, pp. 4015–4026.
- [17] X. Li, H. Ding, H. Yuan, W. Zhang, J. Pang, G. Cheng, K. Chen, Z. Liu, and C. C. Loy, “Transformer-based visual segmentation: A survey,” *IEEE Transactions on Pattern Analysis and Machine Intelligence*, 2024.
- [18] X. Wang, S. Li, K. Kallidromitis, Y. Kato, K. Kozuka, and T. Darrell, “Hierarchical open-vocabulary universal image segmentation,” *Advances in Neural Information Processing Systems*, vol. 36, 2024.
- [19] S. Kazemzadeh, V. Ordonez, M. Matten, and T. Berg, “Referitgame: Referring to objects in photographs of natural scenes,” in *Proceedings of the 2014 conference on empirical methods in natural language processing (EMNLP)*, 2014, pp. 787–798.
- [20] T.-Y. Lin, M. Maire, S. Belongie, J. Hays, P. Perona, D. Ramanan, P. Dollár, and C. L. Zitnick, “Microsoft coco: Common objects in context,” in *Computer Vision—ECCV 2014: 13th European Conference, Zurich, Switzerland, September 6–12, 2014, Proceedings, Part V 13*. Springer, 2014, pp. 740–755.
- [21] Y. Zhan, Z. Xiong, and Y. Yuan, “Rsvg: Exploring data and models for visual grounding on remote sensing data,” *IEEE Transactions on Geoscience and Remote Sensing*, vol. 61, pp. 1–13, 2023.
- [22] S. Huang, T. Hui, S. Liu, G. Li, Y. Wei, J. Han, L. Liu, and B. Li, “Referring image segmentation via cross-modal progressive comprehension,” in *Proceedings of the IEEE/CVF conference on computer vision and pattern recognition*, 2020, pp. 10488–10497.
- [23] Z. Hu, G. Feng, J. Sun, L. Zhang, and H. Lu, “Bi-directional relationship inferring network for referring image segmentation,” in *Proceedings of the IEEE/CVF conference on computer vision and pattern recognition*, 2020, pp. 4424–4433.
- [24] S. Liu, T. Hui, S. Huang, Y. Wei, B. Li, and G. Li, “Cross-modal progressive comprehension for referring segmentation,” *IEEE Transactions on Pattern Analysis and Machine Intelligence*, vol. 44, no. 9, pp. 4761–4775, 2021.
- [25] S. Lei, X. Xiao, T. Zhang, H.-C. Li, Z. Shi, and Q. Zhu, “Exploring fine-grained image-text alignment for referring remote sensing image segmentation,” *IEEE Transactions on Geoscience and Remote Sensing*, 2024.
- [26] S. Ha, C. Kim, D. Kim, J. Lee, S. Lee, and J. Lee, “Finding nemo: Negative-mined mosaic augmentation for referring image segmentation,” in *European Conference on Computer Vision*. Springer, 2024, pp. 121–137.
- [27] Y. Yang, C. Ma, J. Yao, Z. Zhong, Y. Zhang, and Y. Wang, “Remember: Referring image segmentation with mamba twister,” in *European Conference on Computer Vision*. Springer, 2024, pp. 108–126.
- [28] Y. Wang, J. Ni, Y. Liu, C. Yuan, and Y. Tang, “Iterprime: Zero-shot referring image segmentation with iterative grad-cam refinement and primary word emphasis,” *arXiv preprint arXiv:2503.00936*, 2025.
- [29] J. Huang, Z. Xu, T. Liu, Y. Liu, H. Han, K. Yuan, and X. Li, “Densely connected parameter-efficient tuning for referring image segmentation,” *arXiv preprint arXiv:2501.08580*, 2025.
- [30] H. Nguyen-Truong, E.-R. Nguyen, T.-A. Vu, M.-T. Tran, B.-S. Hua, and S.-K. Yeung, “Vision-aware text features in referring image segmentation: From object understanding to context understanding,” in *2025 IEEE/CVF Winter Conference on Applications of Computer Vision (WACV)*. IEEE, 2025, pp. 4988–4998.
- [31] P. Yue, J. Lin, S. Zhang, J. Hu, Y. Lu, H. Niu, H. Ding, Y. Zhang, G. Jiang, L. Cao *et al.*, “Adaptive selection based referring image segmentation,” in *Proceedings of the 32nd ACM International Conference on Multimedia*, 2024, pp. 1101–1110.
- [32] X. Lai, Z. Tian, Y. Chen, Y. Li, Y. Yuan, S. Liu, and J. Jia, “Lisa: Reasoning segmentation via large language model,” in *Proceedings of the IEEE/CVF Conference on Computer Vision and Pattern Recognition*, 2024, pp. 9579–9589.
- [33] Z. Ren, Z. Huang, Y. Wei, Y. Zhao, D. Fu, J. Feng, and X. Jin, “Pixellm: Pixel reasoning with large multimodal model,” in *Proceedings of the IEEE/CVF Conference on Computer Vision and Pattern Recognition*, 2024, pp. 26374–26383.
- [34] C. Yan, H. Wang, S. Yan, X. Jiang, Y. Hu, G. Kang, W. Xie, and E. Gavves, “Visa: Reasoning video object segmentation via large language models,” in *European Conference on Computer Vision*. Springer, 2024, pp. 98–115.
- [35] R. Li, K. Li, Y.-C. Kuo, M. Shu, X. Qi, X. Shen, and J. Jia, “Referring image segmentation via recurrent refinement networks,” in *Proceedings of the IEEE Conference on Computer Vision and Pattern Recognition*, 2018, pp. 5745–5753.
- [36] Y. Jing, T. Kong, W. Wang, L. Wang, L. Li, and T. Tan, “Locate then segment: A strong pipeline for referring image segmentation,” in *Proceedings of the IEEE/CVF Conference on Computer Vision and Pattern Recognition*, 2021, pp. 9858–9867.
- [37] F. Liu, Y. Liu, Y. Kong, K. Xu, L. Zhang, B. Yin, G. Hancke, and R. Lau, “Referring image segmentation using text supervision,” in *Proceedings of the IEEE/CVF International Conference on Computer Vision*, 2023, pp. 22124–22134.
- [38] L. Ye, M. Roohan, Z. Liu, and Y. Wang, “Cross-modal self-attention network for referring image segmentation,” in *Proceedings of the IEEE/CVF conference on computer vision and pattern recognition*, 2019, pp. 10502–10511.
- [39] A. Vaswani, “Attention is all you need,” *Advances in Neural Information Processing Systems*, 2017.
- [40] Z. Yang, J. Wang, Y. Tang, K. Chen, H. Zhao, and P. H. Torr, “Lavt: Language-aware vision transformer for referring image segmentation,” in *Proceedings of the IEEE/CVF Conference on Computer Vision and Pattern Recognition*, 2022, pp. 18155–18165.
- [41] Z. Yang, W. Zhang, Q. Li, W. Ni, J. Wu, and Q. Wang, “C 2 net: Road extraction via context perception and cross spatial-scale feature interaction,” *IEEE Transactions on Geoscience and Remote Sensing*, 2024.
- [42] Z. Yang, Q. Li, Y. Yuan, and Q. Wang, “Hcnet: Hierarchical feature aggregation and cross-modal feature alignment for remote sensing image captioning,” *IEEE Transactions on Geoscience and Remote Sensing*, 2024.
- [43] Z. Liu, Y. Lin, Y. Cao, H. Hu, Y. Wei, Z. Zhang, S. Lin, and B. Guo, “Swin transformer: Hierarchical vision transformer using shifted windows,” in *Proceedings of the IEEE/CVF international conference on computer vision*, 2021, pp. 10012–10022.
- [44] J. Devlin, “Bert: Pre-training of deep bidirectional transformers for language understanding,” *arXiv preprint arXiv:1810.04805*, 2018.